

## Exploration of the limits on charged-lepton-specific forces

Christopher A. Hawkins and Martin L. Perl

Stanford Linear Accelerator Center, Stanford University, Stanford, California 94309

(Received 17 February 1989)

This paper explores the present experimental limits on the existence of a hypothetical force which would only couple to charged leptons; the neutral particle carrying the force having a mass greater than several  $\text{MeV}/c^2$ . We consider limits from data on  $g_e - 2$ ,  $g_\mu - 2$ , electron beam-dump experiments,  $e^+ + e^- \rightarrow e^+ + e^-$ ,  $e^+ + e^- \rightarrow \mu^+ + \mu^-$ , and  $e^+ + e^- \rightarrow \tau^+ + \tau^-$ . Our purpose is to provide a basis for design of future experiments which would be more sensitive to the existence of a charged-lepton-specific force or other unknown phenomena connected to charged leptons.

### I. INTRODUCTION

The known forces which act on leptons (electroweak and gravitational) also act on quarks and other particles. Similarly, proposed interactions involving leptons, the Higgs-particle interaction for example, are also proposed for quarks. Therefore, most searches for new forces have depended upon quarks partaking in that force, even if a final-lepton signature is required. Such searches are irrelevant for a new force which acts only on leptons: a lepton-specific force. In this paper we describe some present experimental limits on the existence and properties of lepton-specific forces *which couple only to charge leptons*. We show that the limits are least imposing when the mass of the particle carrying the force is larger than about  $20 \text{ MeV}/c^2$ . This leads us to describe possible experiments which could probe further into the question of the existence of a force coupling to charged leptons. We have two interests in such experiments.

One interest comes from puzzling over the peculiar properties of the known lepton compared to the known quarks. Unlike the quarks, the two masses in a lepton doublet are very different; indeed, the neutrino mass may be zero. Unlike the quarks, there is no evidence for generation mixing:  $\mu$ -lepton-number conservation holds to at least  $10^{-10}$ ,  $\tau$ -lepton-number conservation holds to at least  $10^{-4} - 10^{-5}$ . Might another peculiarity of the leptons be that there is a force associated only with charged leptons? The latter might be related to the disparate masses problem.

Our second interest comes from a desire to carry out precise and sensitive measurements at high energy which do not involve complicated or poorly understood properties of quarks. Such measurements must either not involve hadrons or only involve hadrons in a well-understood way. Some electron-positron collision reactions meet these criteria and have been carefully studied:

$$e^+ + e^- \rightarrow e^+ + e^-, \quad e^+ + e^- \rightarrow l^+ + l^-, \quad l = \mu, \tau.$$

Other reactions which meet these criteria are

$$\gamma + p \rightarrow l^+ + l^- + p, \quad l = e, \mu,$$

$$e + p \rightarrow l^+ + l^- + e + p, \quad l = e, \mu.$$

The comparison of the precision and sensitivity of different measurements requires a hypothesis as to the unknown physical phenomenon which might be revealed by increased precision or sensitivity. We use the hypothesis of a force coupling only to charged leptons, and a model described next.

In this model the force is carried by a particle called  $\lambda$  of mass  $m_\lambda$ ;  $\lambda$  is neutral and does not change lepton number (Sec. II). To get a feeling for the extent of present limits,  $\lambda$  is allowed to be a pseudoscalar or a vector particle.

In describing current limits on a lepton-specific force we will sometimes make use of results from axion and Higgs-particle search experiments. This is done in Sec. III where the limits are recounted from the comparison of the measurements of  $g_e - 2$  and  $g_\mu - 2$  with theory. In Sec. IV we describe additional limits when  $m_\lambda$  is less than about  $20 \text{ MeV}/c^2$ ; these limits are obtained from electron beam-dump experiments. Additional limits for larger values of  $m_\lambda$  are obtained in Sec. V from measurements on the reactions

$$e^+ + e^- \rightarrow e^+ + e^-, \quad \mu^+ + \mu^-, \quad \tau^+ + \tau^-.$$

Our interest is in direct searches for a force carried by a  $\lambda$  with a mass greater than about  $20 \text{ MeV}/c^2$ . Astrophysical considerations<sup>1</sup> are not of use in this case, although very restrictive limits can be obtained for smaller values of  $m_\lambda$  (less than about  $1 \text{ MeV}/c^2$ ). Therefore, we do not discuss limits coming from astrophysical observations or calculations.

We conclude in Sec. VI with a discussion of possible future experiments on the existence of a charged-lepton-specific force. The emphasis is on the region of large  $m_\lambda$  because this is the region where the limits discussed in this paper exercise the least constraints.

### II. MODEL, LIMIT PHILOSOPHY, LIFETIME

#### A. Model and limit philosophy

We take the  $\lambda$  to be either a pseudoscalar or vector particle which couples only to charged leptons. Using the subscript  $l$  to represent a charged lepton, the  $\lambda$ -lepton vertex has one of the following forms:

$$\text{pseudoscalar: } -ig_{\lambda l}\bar{\nu}_l\gamma_5 u_l, \quad (1a)$$

$$\text{vector: } -ig_{\lambda l}\bar{\nu}_l\gamma_\mu u_l. \quad (1b)$$

We define  $\alpha_{\lambda l} = g_{\lambda l}^2/4\pi$ .

We do not have a fixed idea as to the dependence of the coupling constants  $g_{\lambda l}$  on the nature or properties of the lepton  $l$ . Unlike the Higgs-particle hypothesis we do not connect  $g_{\lambda l}$  with the lepton mass  $m_l$ . We do not assume relationships inside a set of  $g_{\lambda l}$ 's. Each limit is considered separately and presented on a graph of the type of Fig. 1.

Our philosophy in this paper is to sketch out the approximate pseudoscalar and vector limits on  $\alpha_{\lambda l}$  for various ranges of  $m_\lambda$ . We can use approximate limits, usually the 90%-C.L. limit, because we are not testing a specific theory. Our purpose is to find regions where limits on a lepton-specific force are least constrictive; our goal is to carry out search experiments in some of those regions.

There are two other spin and coupling possibilities: scalar and axial vector. We have not reported on all possibilities because it would make too long and repetitive a paper. With these other possibilities the limits are either less restrictive or about as restrictive as the cases we discuss. A further simplification in our considerations is that we assume there is only one  $\lambda$  particle which couples to a specific lepton. We ignore the possibility that two different  $\lambda$ 's couple to the same lepton; hence, we avoid the complication that effects from the two  $\lambda$ 's weaken or cancel each other.

### B. Lifetime when $m_\lambda > 2m_l$

The  $\alpha_{\lambda l}$ - $m_l$  region of sensitivity of a particular search method usually depends upon the lifetime of the  $\lambda$ ,  $\tau_\lambda$ . The simplest case is when  $\lambda$  couples to just one lepton  $l$  and  $m_\lambda > 2m_l$ . Then<sup>2</sup>

$$\text{pseudoscalar: } \tau_\lambda = \frac{2\hbar}{\alpha_\lambda m_\lambda} \left[ 1 - \frac{4m_l^2}{m_\lambda^2} \right]^{-1/2}, \quad (2a)$$

$$\text{vector: } \tau_\lambda = \frac{3\hbar}{\alpha_\lambda m_\lambda} \left[ 1 - \frac{4m_l^2}{m_\lambda^2} \right]^{-1/2} \left[ 1 + \frac{2m_l^2}{m_\lambda^2} \right]^{-1}, \quad (2b)$$

where  $\hbar = 6.6 \times 10^{-22}$  s MeV and  $m_\lambda$  is in MeV.

In most searches the crucial parameter is not  $\tau_\lambda$ , but the decay length,  $L_d = c\gamma_\lambda\tau_\lambda$ . Electron beam-dump experiments in which the  $\lambda$  is directly detected require  $L_d$  larger than tens or hundreds of meters. Experiments which require the  $\lambda$  to leave a production target before decaying require  $L_d$  larger than millimeters or centimeters.

### C. Lifetime when $m_\lambda < 2m_l$

Suppose  $\lambda$  couples to only one lepton, the charged lepton  $l$ , and  $m_\lambda < 2m_l$ . Then the dominant decay mode for the pseudoscalar is

$$\lambda \rightarrow \gamma + \gamma \quad (3a)$$

through a virtual  $l$  loop. The lifetime is<sup>3</sup>

$$\tau_\lambda \approx \frac{16\pi^2\hbar}{\alpha^2\alpha_{\lambda l}m_\lambda} \left[ \frac{m_l}{m_\lambda} \right]^2. \quad (3b)$$

Comparing Eq. (3b) to Eq. (2a), the lifetime is much larger because of the factor  $\alpha^{-2}(m_l/m_\lambda)^2$ .

If  $\lambda$  is a vector it cannot decay to two  $\gamma$ 's. The decay mode  $\lambda \rightarrow 3\gamma$  will have a lifetime longer than that in Eq. (3b) by a factor of about 1000.

### III. LIMITS FROM $g_e - 2$ AND $g_\mu - 2$

A classic activity in atomic and particle physics is to search for new physical phenomena by comparing measurements of  $g_e - 2$  and  $g_\mu - 2$  with calculations. We need only copy the very useful formulas from Ref. 2. In this section we give  $\alpha_{\lambda l}$  vs  $m_\lambda$  limits for the cases of  $\lambda$  scalar or axial vector as well as the cases we use throughout the paper of  $\lambda$  pseudoscalar or vector. Using  $\alpha_l = (g_l - 2)/2$  with  $l = e$  or  $\mu$ , we define

$$\Delta a_l = a_l(\text{measured}) - a_l(\text{calculated}) \quad (4a)$$

and

$$\Delta a_l = \alpha_{\lambda l} K(r)/2\pi. \quad (4b)$$

Here  $r = (m_\lambda/m_l)^2$ . The function  $K(r)$  depends on the nature of  $\lambda$ . The values of  $K(r)$  at small and large values of  $r$  are instructive: limit as  $r = m_\lambda^2/m_l^2 \rightarrow 0$ ,

$$\begin{aligned} \text{pseudoscalar: } K &\rightarrow \frac{1}{2}, \quad \text{vector: } K \rightarrow 1, \\ \text{scalar: } K &\rightarrow -\frac{3}{2}, \quad \text{axial vector } K \rightarrow 4 \ln(r); \end{aligned} \quad (4c)$$

limit as  $r = m_\lambda^2/m_l^2 \rightarrow \infty$ ,

$$\begin{aligned} \text{pseudoscalar: } K &\rightarrow (1/r)\ln(r), \\ \text{vector: } K &\rightarrow 2/(3r), \\ \text{scalar: } K &\rightarrow -(1/r)\ln(r), \\ \text{axial vector: } K &\rightarrow -10/(3r). \end{aligned} \quad (4d)$$

The limits on  $\Delta a_l$  are not symmetric. From Ref. 4,

$$\begin{aligned} \Delta a_e &= (-1.11 \pm 1.28) \times 10^{-10}, \\ \Delta a_\mu &= (3.9 \pm 8.7) \times 10^{-9}. \end{aligned}$$

The 90%-C.L. limits are

$$\begin{aligned} \Delta a_e &< +0.53 \times 10^{-10}, \quad \Delta a_e > -2.75 \times 10^{-10}, \\ \Delta a_n &< +1.50 \times 10^{-8}, \quad \Delta a_\mu > -0.72 \times 10^{-8}. \end{aligned} \quad (5)$$

The limits on  $\Delta a_l$  in Eq. (5) lead to the excluded regions in Fig. 1. When  $m_\lambda \lesssim m_l$ , the upper limit on  $\alpha_\lambda$  is of the order of  $2\pi\Delta a_l$ , a drastic constraint on  $\alpha_{\lambda l}$ . This constraint weakens when  $m_\lambda \gg m_l$ , the upper limit increases approximately as  $m_\lambda^2$ . As stated in Sec. II A, we assume only one  $\lambda$  couples to a lepton.

The limits on  $\alpha_\lambda$  provided by  $\Delta a_l$  are a foundation on which we erect other limits from other data and searches (Secs. IV and V). Note that although  $\Delta a_\mu$  is about 100

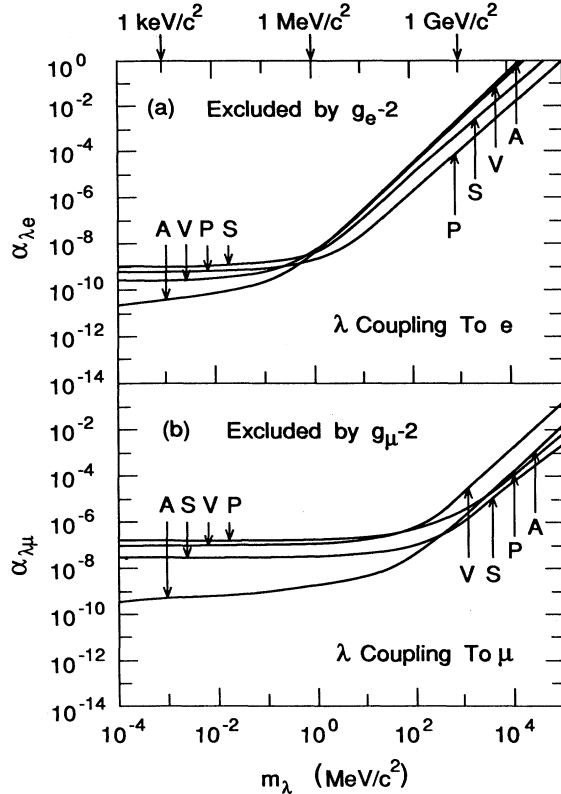


FIG. 1. Upper limits on  $\alpha_{\lambda l}$  set by  $g_l-2$  measurements for (a)  $l$ =electron and (b)  $l$ =muon.  $A$ =axial vector,  $V$ =vector,  $P$ =pseudoscalar,  $S$ =scalar.

times larger than  $\Delta a_e$ , at large values of  $m_\lambda$  there is a stronger constraint on  $\alpha_{\lambda\mu}$  compared to  $\alpha_{\lambda e}$  due to the effect of the muon mass.

#### IV. LIMITS FROM ELECTRON BEAM-DUMP EXPERIMENTS

##### A. $0 \leq m_\lambda < 2m_e$

Two electron beam-dump experiments,<sup>5,6</sup> schematically described by Fig. 2 have been carried out at SLAC. A beam of 20-GeV electrons is dumped into a target containing at least several radiation lengths. Directly downstream of the target, a distance  $D$ , is a track-detecting and electromagnetic-shower-detecting, thick plate chamber. The distance  $D$  is partially filled with shielding. In the experiment of Rothenberg,<sup>5</sup>  $D$  was about 60 m, the detector consisted of four optical spark chambers with thick aluminum plates, and the total number of effective radiation lengths in the detector was about 9.4. In the experiment of Bjorken *et al.*,<sup>6</sup>  $D$  was about 400 m, the detector consisted of aluminum or iron plates interleaved with multiwire proportional chambers, and the total number of effective radiation lengths was about 4. In the former experiment, the physicists looked for events which might be neutrino interactions, these events consisting of one or more charged particles. Electromagnetic showers of sufficient energy would also have been detect-

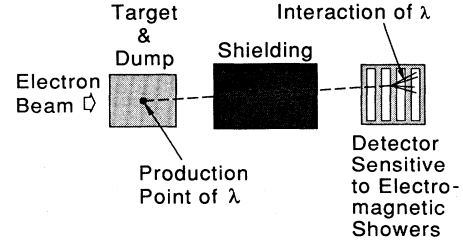


FIG. 2. Schematic of electron beam-dump experiments which set limits on  $\alpha_{\lambda e}$  and  $m_\lambda$  when  $m_\lambda < 2m_e$ .

ed. In the latter experiment, the physicists specifically looked for electromagnetic showers. Neither experiment reported any unexplained source of electromagnetic showers.

We can interpret the null results of these experiments for our purposes by noting that the  $\lambda$  could be produced by the process, Fig. 3(a),

$$e^- + \text{nucleus} \rightarrow e^- + \lambda + \text{nucleus or nucleons}, \quad (6a)$$

analogous to electron bremsstrahlung. Some  $\lambda$ 's which reach the detector and have sufficient energy will interact with the material in the detector through the process, Fig. 3(b),

$$\lambda + \text{nucleus} \rightarrow e^+ + e^- + \text{nucleus or nucleons}, \quad (6b)$$

analogous to photoproduction of  $e^+e^-$  pairs.

An order-of-magnitude calculation shows that this is a sensitive search method for  $\lambda$  coupling to an  $e$  when  $m_\lambda < 2m_e$ . This mass restriction combined with the  $g_e-2$  constraint in Fig. 1(a) means that the sensitivity of the beam-dump experiment need only be investigated for  $\alpha_{\lambda e} < 3 \times 10^{-9}$ . The lifetime for a pseudoscalar  $\lambda$ , Eq. 3(b), is

$$\tau_\lambda(m_\lambda < 2m_e) > 9 \times 10^{-8} \text{ s}. \quad (7a)$$

We will only consider  $\lambda$ 's with energy greater than 2 GeV; hence, the decay length is

$$D_\lambda(m_\lambda < 2m_e) > 5 \times 10^4 \text{ m}. \quad (7b)$$

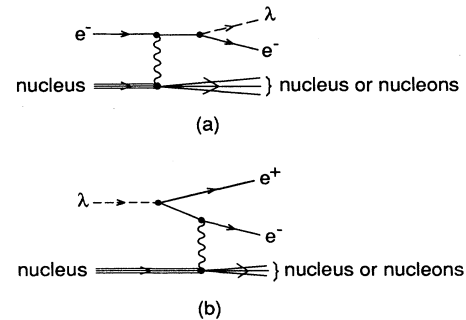


FIG. 3. Diagrams for (a)  $e^- + \text{nucleus} \rightarrow e^- + \lambda + \text{nucleus or nucleons}$  and (b)  $\lambda + \text{nucleus} \rightarrow e^+ + e^- + \text{nucleus or nucleons}$ .

This decay length is much larger than the target to detector distance in either experiment. Thus both experiments are applicable. Although the experiment of Rothenberg<sup>5</sup> and Donnelly *et al.*<sup>5</sup> is in principle more sensitive than that of Bjorken *et al.*,<sup>6</sup> we will analyze only the experiment of Bjorken *et al.*,<sup>6</sup> because we have been able to discuss the detector sensitivity with one of the experimenters.<sup>7</sup>

No electromagnetic showers of greater than 2-GeV energy were found in 4 radiation lengths of the detector when a total of 30 C of 20-GeV electrons were used. We show here the calculation of the limit on  $\alpha_{\lambda e}$  for  $\lambda$  being massless and a vector. The pseudoscalar case and mass dependence are related to the massless vector case using relations given by Tsai.<sup>8</sup>

An EGS (Ref. 9) shower simulation gives the number of  $\lambda$ 's produced in the dump that are within the detector acceptance to be  $3.76 \alpha_{\lambda e} / \alpha$   $\lambda$ 's per incident electron. For  $C$  coulombs, the number of produced  $\lambda$ 's is

$$N_{\lambda} \sim 2.3 \times 10^{19} C \alpha_{\lambda e} / \alpha .$$

The shielding contains about 1300 radiation lengths, but since we are only concerned with  $\alpha_{\lambda e} < 10^{-8}$  because of the  $g_e - 2$  constraint, there is negligible attenuation of  $\lambda$ 's in the shielding. The probability that a  $\lambda$  of 2 GeV or more energy produces a shower in an  $N_{\text{rad}}$ -radiation-length detector is  $\frac{7}{9} N_{\text{rad}} (\alpha_{\lambda e} / \alpha)$ . Therefore, the number of showers expected is

$$N_{\text{shower}} = 2.3 \times 10^{19} C \frac{7}{9} N_{\text{rad}} (\alpha_{\lambda e} / \alpha)^2 . \quad (8a)$$

Taking the upper limit on  $N_{\text{shower}}$  as 2.3, with  $C = 30$  and  $N_{\text{rad}} = 4$ ,

$$\alpha_{\lambda e} \lesssim 2.4 \times 10^{-13} . \quad (8b)$$

Thus for  $m_{\lambda} < 2m_e$ , our interpretation of these beam-dumped experiments decreases the upper limit on  $\alpha_{\lambda e}$  from about  $10^{-8}$  to about  $2 \times 10^{-13}$ . These limits as a function of  $m_{\lambda}$  are shown later in Fig. 5.

Once  $m_{\lambda} > 2m_e$  the  $\lambda$  lifetime becomes too short to use our interpretation of this experiment. But at this boundary another set of search experiments can be used, those connected with the possibility of the production of anomalous  $e^+e^-$  pairs in heavy-ion collisions.

### B. $2m_e < m_{\lambda} \lesssim 15 \text{ MeV}/c^2$

In the past decade there has been continuing but confusing evidence<sup>10</sup> that there is anomalous production of  $e^+e^-$  pairs when heavy ions such as Th and U collide. When the kinetic energy of the incident ion is about the energy required to overcome the Coulomb barrier between the nuclei, there appear to be peaks in the  $e^+e^-$  mass spectrum between about 1.5 and 1.8  $\text{MeV}/c^2$ . A great deal of theoretical and experimental research has involved the hypothesis that the  $e^+e^-$  pair are the decay products of a neutral particle produced in the heavy-ion collision, which we call  $\lambda$ .

One area of experimental research has looked for the  $\lambda$  through the sequence

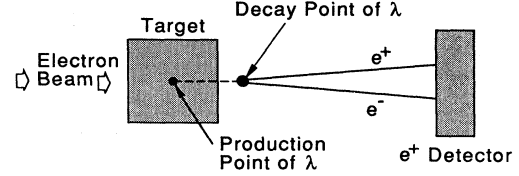


FIG. 4. Schematic of electron beam-dump experiments which set limits on  $\alpha_{\lambda e}$  and  $m_{\lambda}$  when  $m_{\lambda} > 2m_e$ .

$$e^- + \text{nucleus} \rightarrow e^- + \lambda + \text{nucleus or nucleons} , \quad (9a)$$

$$\lambda \rightarrow e^+ + e^- . \quad (9b)$$

The reaction in Eq. (9a) is the same as that in Eq. (6a) and Fig. 3(a). Tsai,<sup>8</sup> Olsen,<sup>11</sup> and Holvik and Olsen<sup>12</sup> give the theory and cross sections for this reaction. The decay process, Eq. (9b), must take place outside the production target, Fig. 4, setting a lower limit on the  $\lambda$  lifetime. As shown in Fig. 4, in these experiments the existence of the  $\lambda$  would be demonstrated by an excess of positrons in the forward direction.

Most of the searches<sup>13-15</sup> have used electron beams. One search<sup>16</sup> analyzed data from a proton beam-dump experiment; high-energy electrons are produced in the dump through the sequence

$$p + \text{nucleon} \rightarrow \pi^0 + \dots , \quad \pi^0 \rightarrow \gamma + \gamma , \quad (10)$$

$$\gamma + \text{nucleus} \rightarrow e^+ + e^+ + \dots .$$

The results of all these searches<sup>13-16</sup> were null.

Davies<sup>17</sup> has combined the limits from Refs. 13-16 and from an earlier electron beam-dump search for axions.<sup>18</sup> We apply the same limits to a pseudoscalar  $\lambda$  in Fig. 5. We also show in Fig. 5 the excluded region from the beam-dump experiments discussed in Sec. IV A. Thus the excluded region from Sec. IV A is extended to larger values of  $m_{\lambda}$ , to about 15  $\text{MeV}/c^2$ . In a narrow range of  $m_{\lambda}$ , the upper limit on  $\alpha_{\lambda e}$  is reduced to  $10^{-14}$ .

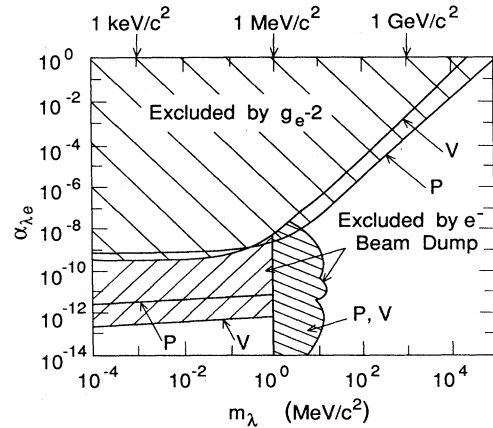


FIG. 5. Excluded regions of  $\alpha_{\lambda e}$  vs  $m_{\lambda}$  from considerations in Secs. III and IV.  $V$  = vector,  $P$  = pseudoscalar.

A new electron beam-dump experiment has been proposed<sup>19</sup> for Fermilab.

There is no calculation of the limits imposed by these experiments if  $\lambda$  is a vector particle. In that case the  $\lambda$  momentum spectrum is similar to the  $\gamma$  momentum spectrum from

$$e^- + \text{nucleus} \rightarrow e^- + \gamma + \text{nucleus or nucleons} \quad (11a)$$

and the background from

$$\gamma + \text{nucleus} \rightarrow e^- + e^+ + \text{nucleus} \quad (11b)$$

is more serious. However Riordan<sup>20</sup> pointed out to us that the production cross section for the reaction in Eq. (9a) is larger for a vector  $\lambda$  compared to a pseudoscalar  $\lambda$ . Riordan concludes<sup>20</sup> that the  $\alpha_{\lambda e} - m_\lambda$  excluded region is about the same for the two types of  $\lambda$ . Hence, we use these beam-dump limits, Fig. 5, for a vector  $\lambda$ .

The type of electron beam-dump search discussed in this section becomes less sensitive as  $m_\lambda$  increases above 15 MeV/ $c^2$ . The production cross section decreases.<sup>8</sup> Furthermore, the decay length is proportional to  $m_\lambda^{-2}$  for fixed  $\alpha_{\lambda e}$  and fixed energy; hence, a thinner target must be used. Therefore, other search methods must be used for large values of  $m_\lambda$ .

## V. LIMITS FROM $e^+e^-$ COLLISION DATA

### A. $e^+ + e^- \rightarrow e^+ + e^-$

#### 1. Vector $\lambda$

The Feynman diagrams in Fig. 6 are, for Bhabha scattering,

$$e^+ + e^- \rightarrow e^+ + e^-, \quad (12)$$

through both  $\gamma$  and  $\lambda$  exchange. If  $\lambda$  is a vector particle the cross section is given by the formula for  $\gamma$  and  $Z^0$  exchange<sup>21</sup> with the  $Z^0$ 's axial-vector coupling parameter set to 0.

In the barycentric system

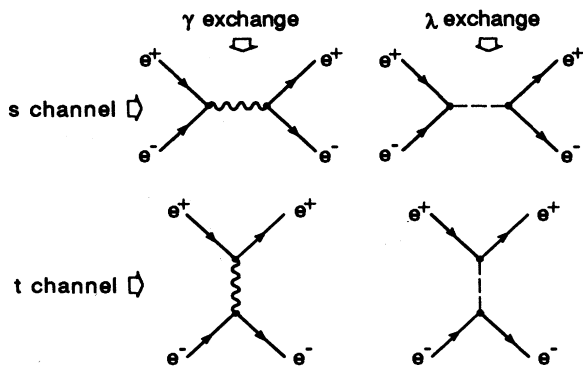


FIG. 6. Feynman diagrams for the process  $e^+ + e^- \rightarrow e^+ + e^-$  taking place through  $\gamma$  and  $\lambda$  exchange.

$$\frac{d\sigma(e^+e^- \rightarrow e^+e^-)}{d\cos\theta} = \frac{\pi\alpha^2}{s} (f_{\gamma\gamma} + x f_{\gamma\lambda} + x^2 f_{\lambda\lambda}), \quad (13a)$$

$$x = \frac{\alpha_{\lambda e}}{\alpha_\gamma}, \quad (13a)$$

where  $f_{\gamma\gamma}$ ,  $f_{\gamma\lambda}$ , and  $f_{\lambda\lambda}$  are the contributions from the product of  $\gamma$ - $\gamma$ ,  $\gamma$ - $\lambda$ , and  $\lambda$ - $\lambda$  amplitudes. Specifically,

$$f_{\gamma\gamma} = \left[ \frac{s^2 + u^2}{t^2} + \frac{2u^2}{st} + \frac{t^2 + u^2}{s^2} \right], \quad (13b)$$

$$f_{\gamma\lambda} = 2 \left[ \left[ \frac{s^2 + u^2}{t^2} \right] (R_t)_{\text{real}} + \frac{u^2}{st} (R_t + R_s)_{\text{real}} + \left[ \frac{t^2 + u^2}{s^2} \right] (R_s)_{\text{real}} \right], \quad (13c)$$

$$f_{\lambda\lambda} = \left[ \left[ \frac{s^2 + u^2}{t^2} \right] |R_t|^2 + \frac{2u^2}{st} (R_s R_t)_{\text{real}} + \left[ \frac{t^2 + u^2}{s^2} \right] |R_s|^2 \right], \quad (13d)$$

where

$$t = -s(1 - \cos\theta)/2, \quad u = -s(1 + \cos\theta)/2, \quad (13e)$$

$$R_t = t/(t - m_\lambda^2 + i\Gamma_\lambda m_\lambda), \quad R_s = s/(s - m_\lambda^2 + i\Gamma_\lambda m_\lambda).$$

We found that the most sensitive search for a nonzero  $x$  uses high-energy  $e^+e^-$  storage-ring data on the partial total cross section

$$\sigma'(e^+e^- \rightarrow e^+e^-) = \int_{-c}^c \left[ \frac{d\sigma(e^+e^- \rightarrow e^+e^-)}{d\cos\theta} \right] d\cos\theta, \quad (14a)$$

where the limits of integration  $\pm c$  depend on the experiment. The prime indicates the cross section is for part of the  $\cos\theta$  range. From Eqs. (13),

$$\sigma'(e^+e^- \rightarrow e^+e^-) = \sigma'_{\gamma\gamma} + x\sigma'_{\gamma\lambda} + x^2\sigma'_{\lambda\lambda}. \quad (14b)$$

Suppose an experiment reports the upper limit

$$\frac{\sigma'_{\text{meas}}(e^+e^- \rightarrow e^+e^-) - \sigma'_{\text{QED}}(e^+e^- \rightarrow e^+e^-)}{\sigma'_{\text{QED}}(e^+e^- \rightarrow e^+e^-)} < \epsilon. \quad (15a)$$

Then in our model,

$$x^2 \left[ \frac{\sigma'_{\lambda\lambda}}{\sigma'_{\gamma\gamma}} \right] + x \left[ \frac{\sigma'_{\gamma\lambda}}{\sigma'_{\gamma\gamma}} \right] < \epsilon \quad (15b)$$

gives the limit on  $x$ . Using

$$r_2 = \sigma'_{\lambda\lambda}/\sigma'_{\gamma\gamma}, \quad r_1 = \sigma'_{\gamma\lambda}/\sigma'_{\gamma\gamma}, \quad r_2 x_{\text{lim}}^2 + r_1 x_{\text{lim}} = \epsilon. \quad (16)$$

The sizes of  $r_1$  and  $r_2$  and hence the relation of the  $x_{\text{lim}}$ 's to  $\epsilon$  depends on  $m_\lambda$ . When  $|s - m_\lambda^2| \sim m_\lambda \Gamma_\lambda$  the  $s$ -channel resonance in  $R_s$  dominates  $\sigma'$ , and the deviation

from pure photon exchange will depend on  $x^2$ . Otherwise the  $\gamma$ - $\lambda$  interference term,  $r_1 x$  in Eq. (16), is most important and the deviation depends on  $x$ .

In looking for a deviation from pure photon exchange it is crucial to examine how the luminosity was determined in a measurement of  $\sigma'(e^+e^- \rightarrow e^+e^-)$ . The use of large-angle  $e^+e^- \rightarrow e^+e^-$  scattering to determine the luminosity negates the search for a deviation. We have used the comparison of  $\sigma'(e^+e^- \rightarrow e^+e^-)$  and  $\sigma'(e^+e^- \rightarrow \gamma\gamma)$  of Derrick *et al.*<sup>22</sup> Using data from the High Resolution Spectrometer (HRS) detector at the SLAC  $e^+e^-$  storage ring PEP they give

$$\left[ \frac{\sigma'(e^+e^- \rightarrow e^+e^-)}{\sigma'(e^+e^- \rightarrow \gamma\gamma)} \right]_{\text{meas}} / \left[ \frac{\sigma'(e^+e^- \rightarrow e^+e^-)}{\sigma'(e^+e^- \rightarrow \gamma\gamma)} \right]_{\text{QED}} = 0.993 \pm 0.009 \pm 0.008, \quad (17)$$

where  $c$  in Eq. (14a) is 0.55, and QED means the theory is pure quantum electrodynamics calculated to third order in  $\alpha$ . In our model  $\lambda$  does not enter into the reaction  $e^+ + e^- \rightarrow \gamma + \gamma$  in lowest order; hence, we use Eq. (17) to set the deviations allowed in  $e^+ + e^- \rightarrow e^+ + e^-$  due to the presence of the  $\lambda$ . Following our philosophy of giving approximate, exploratory limits we add quadratically the statistical and systematic errors to give a measure of the allowed deviation. The 90%-C.L. limit is

$$\epsilon = 0.008. \quad (18)$$

Using Eqs. (13), (14), and (16) we obtain the limits on  $\alpha_{\lambda e}$  in Fig. 7.

The width of resonance at  $\sqrt{s} = 29$  GeV is set mostly by the variation in the beam energy of PEP over the

course of several years' data acquisition. We took the variation in the  $\sqrt{s}$  to be  $\pm 0.002\sqrt{s}$ . Values of  $\alpha_{\lambda e}$  as small as  $10^{-3} - 4 \times 10^{-5}$  are excluded by the measurement of Derrick *et al.*<sup>22</sup> At 29 GeV the  $\alpha_{\lambda e}$  limit reaches below  $10^{-5}$ , but these values are dependent on our uncertain estimation of the experimental resonance width.

The limits on  $\alpha_{\lambda e}$  for  $m_\lambda > 29$  GeV might be further examined through the use of  $e^+e^- \rightarrow e^+e^-$  data from the DESY PETRA or KEK TRISTAN storage rings, but we have not found published data that we could directly use; uncertainties in the luminosity determination negate the advantage of the higher energy. This can certainly be overcome by experimenters who have their own data from these storage rings.

## 2. Pseudoscalar $\lambda$

When  $\lambda$  is pseudoscalar or scalar the Bhabha-scattering differential cross section in the barycentric system is

$$\frac{d\sigma(e^+e^- \rightarrow e^+e^-)}{d\cos\theta} = \frac{\pi\alpha^2}{s} (f_{\gamma\gamma} + x f_{\gamma\lambda} + x^2 f_{\lambda\lambda}). \quad (19a)$$

Here

$$f_{\gamma\gamma} = \left[ \frac{s^2 + u^2}{t^2} + \frac{2u^2}{st} + \frac{t^2 + u^2}{s^2} \right], \quad (19b)$$

$$f_{\gamma\lambda} = - \left[ -\frac{u}{t} (R_s)_{\text{real}} + \frac{u}{s} (R_t)_{\text{real}} \right], \quad (19c)$$

$$f_{\lambda\lambda} = \frac{1}{2} [ |R_t|^2 + (R_s R_t)_{\text{real}} + |R_s|^2 ], \quad (19d)$$

where the notation is described in Eq. (13e).

We again use the limit from Derrick *et al.*,<sup>22</sup> Eq. (18), and the analysis described in Sec. V A 1. The excluded regions of  $\alpha_{\lambda e}$  are given in Fig. 8.

The excluded regions are smaller than the vector case, Fig. 7, because  $r_1$  and  $r_2$  are smaller in the pseudoscalar case compared to the vector case. For example, set  $m_\lambda = 0$ , then

$$\text{pseudoscalar: } r_1 = -0.107, \quad r_2 = 0.214,$$

$$\text{vector: } r_1 = 2.000, \quad r_2 = 1.000.$$

The limits in Fig. 8 also apply to a scalar  $\lambda$ .

$$\text{B. } e^+ + e^- \rightarrow \mu^+ + \mu^-, \tau^+ + \tau^-$$

### 1. Vector $\lambda$

The  $s$ -channel reaction

$$e^+ + e^- \rightarrow l^+ + l^-, \quad l = \mu, \tau \quad (20)$$

provides limits on

$$\alpha_{\lambda e l} = g_{\lambda e} g_{\lambda l} / 4\pi$$

through the diagrams in Fig. 9. The barycentric differential cross section has the simple form

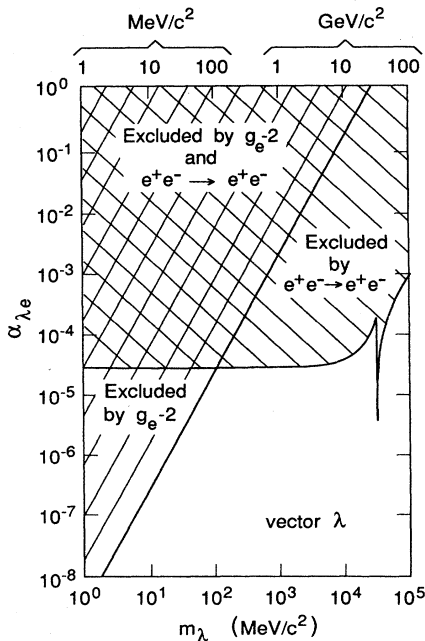


FIG. 7. Limits on  $\alpha_{\lambda e}$  for a vector  $\lambda$  from  $e^+e^- \rightarrow e^+e^-$  at 29 GeV and  $g_e = 2$ .

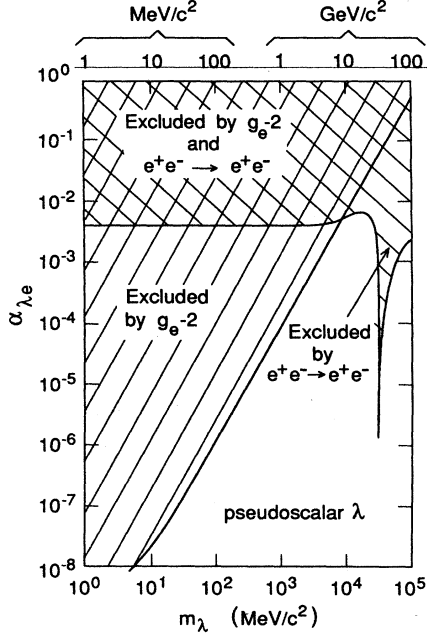


FIG. 8. Limits on  $\alpha_{\lambda e}$  for a pseudoscalar  $\lambda$  from  $e^+e^- \rightarrow e^+e^-$  at 29 GeV and  $g_e - 2$ .

$$\frac{d\sigma}{d\cos\theta} = \frac{\pi\alpha^2\beta}{s} (2 - \beta^2 + \beta^2\cos^2\theta) \times [1 + 2x(R_s)_{\text{real}} + x^2|R_s|^2], \quad (21a)$$

where

$$x = \alpha_{\lambda e l} / \alpha_{\gamma}, \quad R_s = s / (s - m_\lambda^2 + i\Gamma_\lambda m_\lambda) \quad (21b)$$

and  $\beta$  is  $v_l/c$ .

The magnitude of  $d\sigma/d\cos\theta$  is determined in part by the luminosity, which in turn depends upon large-angle Bhabha scattering. As in Sec. V A we define a partial total cross section  $\sigma'$  obtained by integrating  $d\sigma/d\cos\theta$  within the range  $-c < \cos\theta < c$ . The limits on  $x$  are obtained from the ratio

$$\rho(e^+e^- \rightarrow \gamma\gamma) = \frac{\sigma'_{\text{meas}}(e^+e^- \rightarrow l^+l^-) / \sigma'_{\text{meas}}(e^+e^- \rightarrow e^+e^-)}{\sigma'_{\text{QED}}(e^+e^- \rightarrow l^+l^-) / \sigma'_{\text{QED}}(e^+e^- \rightarrow e^+e^-)}.$$

An exact treatment of this ratio requires recognition that  $\sigma'_{\text{meas}}(e^+e^- \rightarrow e^+e^-)$  was used to set limits on  $\alpha_{\lambda e} = g_{\lambda e}^2/4\pi$ . It is sufficient for our purpose to quadratically add the errors in  $\sigma'_{\text{meas}}(e^+e^- \rightarrow e^+e^-)$  to the larger er-

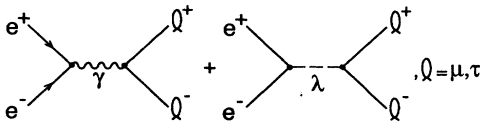


FIG. 9. Feynman diagrams for  $e^+ + e^- \rightarrow \mu^+ + \mu^-, \tau^+ + \tau^-$ .

rors in  $\sigma'_{\text{meas}}(e^+e^- \rightarrow l^+l^-)$  and use the combined error  $\epsilon$ , where

$$\frac{\sigma'_{\text{meas}}(e^+e^- \rightarrow l^+l^-)}{\sigma_{\text{QED}}(e^+e^- \rightarrow l^+l^-)} = 1 + \epsilon. \quad (22)$$

From Eqs. (21) and (22),

$$x_{\text{lim}}^2 |R_s|^2 + 2x_{\text{lim}}(R_s)_{\text{real}} = \epsilon, \quad (23)$$

$$\mu: \epsilon_\mu = 0.038, \quad \tau: \epsilon_\tau = 0.064. \quad (24)$$

The  $\epsilon_\mu$  value comes from the 29-GeV results in Refs. 22 and 23. The  $\epsilon_\tau$  value comes from the 29-GeV results in Ref. 24 and an additional uncertainty due to the problem in understanding the  $\tau$  decay modes.<sup>25</sup> When  $\epsilon_\mu$  or  $\epsilon_\tau$  are inserted in Eq. (23) we obtain the limits in Figs. 10 and 11.

## 2. Pseudoscalar $\lambda$

If  $\lambda$  is pseudoscalar there is no interference between the  $\gamma$ -exchange and  $\lambda$ -exchange amplitudes:

$$\frac{d\sigma}{d\cos\theta} = \frac{\pi\alpha^2\beta}{s} [(2 - \beta^2 + \beta^2\cos^2\theta) + x^2|R_s|^2], \quad (25)$$

where the notation is given in Eq. (21b). The limit on  $\alpha_{\lambda e\mu}$  is given by

$$x_{\text{lim}} r = \sqrt{\epsilon}, \quad (26a)$$

where

$$r = |R_s| / (2 - \beta^2 + \beta^2\cos^2\theta)^{1/2}. \quad (26b)$$

This is for the partial cross section for the range  $-c < \cos\theta < c$ .

The  $\epsilon$  values given in Eq. (24) lead to the upper limits on  $\alpha_{\lambda e\mu}$  in Fig. 10 and on  $\alpha_{\lambda e\tau}$  in Fig. 11.

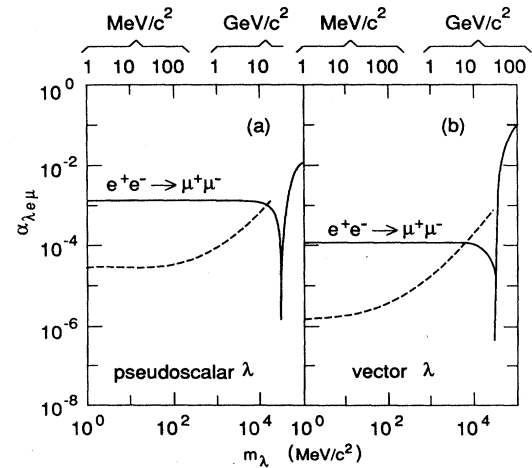


FIG. 10. In (a)  $\lambda$  pseudoscalar and (b)  $\lambda$  vector the solid curve gives the upper limit on  $\alpha_{\lambda e\mu}$  from  $e^+e^- \rightarrow \mu^+\mu^-$ . The dashed curve gives the upper limit on  $\sqrt{\alpha_{\lambda e}\alpha_{\lambda\mu}}$ .

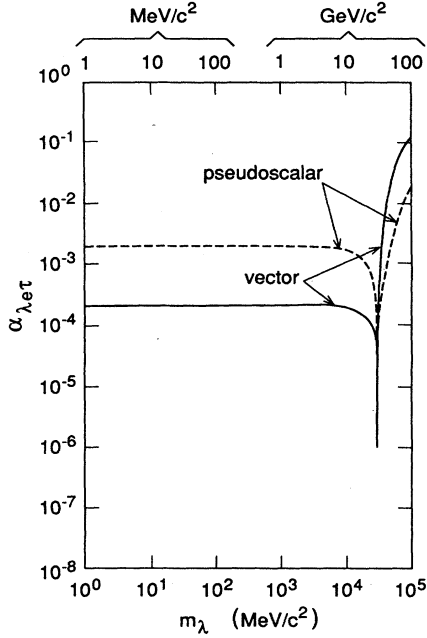


FIG. 11. The curves marked pseudoscalar and vector give the upper limit on  $\alpha_{\lambda e\tau}$  from  $e^+e^- \rightarrow \tau^+\tau^-$  for  $\lambda$  pseudoscalar and  $\lambda$  vector.

### 3. Discussion of $\alpha_{\lambda e\mu}, \alpha_{\lambda e\tau}$

The upper limits in Figs. 10 and 11 on

$$\alpha_{\lambda e l} = g_{\lambda e} g_{\lambda l} / 4\pi \quad (27)$$

do not set limits on  $g_{\lambda l}$  unless we know a connection between  $g_{\lambda e}$  and  $g_{\lambda l}$ . In the special case of  $g_{\lambda e} = 0$ , the upper limit on  $\alpha_{\lambda e l}$  tells us nothing about  $g_{\lambda l}$ . In a model which copies the Higgs-particle hypothesis with  $g_{\lambda l} = (m_l/m_e)g_{\lambda e}$ , the individual upper limits are given by  $\alpha_{\lambda l} = g_{\lambda l}^2/4\pi = (m_l/m_e)\alpha_{\lambda e l}$  and  $\alpha_{\lambda e} = g_{\lambda e}^2/4\pi = (m_e/m_l)\alpha_{\lambda e l}$ .

In Fig. 10 we compare the  $\alpha_{\lambda\mu}$  upper limit (solid curve) with the upper limit on  $\sqrt{\alpha_{\lambda e}\alpha_{\lambda\mu}}$  (dashed curve). The  $\alpha_{\lambda e}$  limit is obtained from  $e^+e^- \rightarrow e^+e^-$  (Sec. IV A); the  $\alpha_{\lambda\mu}$  limit is obtained from  $g_{\mu-2}$  (Sec. III). For much of the range of  $m_\lambda < 29$  GeV, the  $\sqrt{\alpha_{\lambda e}\alpha_{\lambda\mu}}$  upper limits are smaller than the  $\alpha_{\lambda e\mu}$  upper limit.

## VI. SUMMARY AND DISCUSSION

In the spirit of our model we discuss separately the  $e$ ,  $\mu$ , and  $\tau$ . We remark on the limits given in this paper, we point out other existing data that can be examined, and discuss possible future experiments.

### A. Electron-specific forces

#### 1. Remarks on limits and use of other data

Figures 1(a), 7, and 8 summarize the limits on the  $\lambda$ - $e$  system. When  $m_\lambda$  is greater than about 200 MeV/ $c^2$ , the smallest upper bound on  $\alpha_{\lambda e}$  comes from  $e^+e^- \rightarrow e^+e^-$ .

Depending on the properties assumed for  $\lambda$ , the upper bound lies between  $10^{-2}$  and  $10^{-5}$  for most of the  $m_\lambda$  range. Smaller upper bounds occur, of course, at the resonant mass for the data we used,  $m_\lambda = 29$  GeV/ $c^2$ . But such a bound has little use because it only applies to an  $m_\lambda$  mass range about 0.1 GeV/ $c^2$  wide at 29 GeV/ $c^2$ .

The increased sensitivity of the  $e^+e^- \rightarrow e^+e^-$  cross section at the resonance  $m_\lambda = E_{c.m.}$  might be used over a broader mass range by analyzing data required during energy scans. For example, the energy range from about 3 to 6 GeV was scanned at the SLAC storage ring SPEAR (Ref. 26), and from about 30 to 46 GeV was scanned at PETRA (Ref. 21). To use such scan data close attention must be paid to how the large-angle Bhabha scattering was normalized. We have not made such a study.

We are studying<sup>27</sup> data from the SLAC storage ring PEP on the reaction

$$e^+ + e^- \rightarrow e^+ + e^- + e^+ + e^-, \quad (28a)$$

looking for the process

$$e^+ + e^- \rightarrow e^+ + e^- + \lambda, \quad \lambda \rightarrow e^+ + e^- \quad (28b)$$

through detection of an  $e^+e^-$  mass peak at  $m_\lambda$ . Figure 12(a) shows one of the Feynman diagrams for this hypothetical process.

### 2. Possible future experiments

A  $\lambda$  search method analogous to that in Eq. (28b) uses electroproduction on a proton:

$$e^- + p \rightarrow e^- + p + \lambda, \quad \lambda \rightarrow e^+ + e^- \quad (29)$$

Figure 12(b) shows one of the Feynman diagrams. Again the  $\lambda$  would be detected by an  $e^+e^-$  mass peak. In an  $ep$  fixed-target search using an  $e^-$  beam of energy  $E_{\text{beam}}$ , the mass range is limited by  $m_\lambda < \sqrt{2E_{\text{beam}}m_{\text{proton}}}$ . This limit is smaller than the  $m_\lambda < E_{c.m.}$  limit for the  $e^+e^- \rightarrow e^+e^- + \lambda$  process in a storage ring. However the  $ep$  fixed-target search experiment can be designed<sup>28</sup> for a higher effective interaction rate and hence greater sensitivity. The search can also be carried out at the HERA  $ep$  collider now under construction.

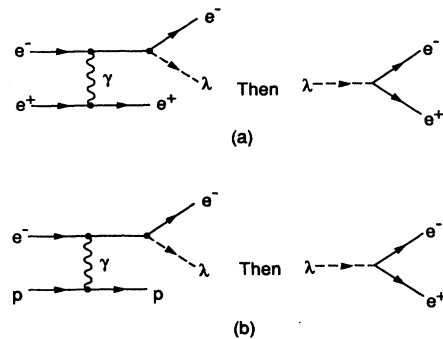


FIG. 12. Examples of Feynman diagrams for (a)  $e^+e^- \rightarrow e^+e^- + \lambda$ ,  $\lambda \rightarrow e^+e^-$ , and (b)  $e^- + p \rightarrow e^- + p + \lambda$ ,  $\lambda \rightarrow e^+e^-$ .



In thinking about possible methods to search for a  $\lambda$  coupled to an  $e$ , one can consider a deliberate energy scan of the  $e^+e^- \rightarrow e^+e^-$  cross section, looking for the resonance at  $E_{c.m.} = m_\lambda$ . The scanning could be done in an  $e^+e^-$  collider or in a fixed-target experiment. Unfortunately, such a scanning search at existing  $e^+e^-$  storage rings would be a long experiment and could not be justified at this time. The mass range in a fixed-target scanning search is limited to  $m_\lambda < \sqrt{2E_{beam}}m_e$ , about 220 MeV/ $c^2$  for the 50-GeV  $e^-$  beam at SLAC. We have not investigated whether such a search could extend into the unexplored regions in Figs. 7 and 8.

## B. Muon-specific forces

### 1. Remarks on limits and use of other data

If the  $\lambda$  couples only to the  $\mu$ , our only limits on  $\alpha_{\lambda\mu}$  come from  $g_\mu - 2$ , Fig. 1(b). As discussed in Sec. III, the larger size of  $m_\mu$  compared to  $m_e$  leads to the limits imposed by  $g_\mu - 2$  extending to larger values of  $m_\lambda$ . Comparing Fig. 7 for  $\alpha_{\lambda e}$  with Fig. 1(b) for  $\alpha_{\lambda\mu}$ , one sees that most of the  $\alpha_{\lambda e} - m_\lambda$  region excluded by  $e^+e^- \rightarrow e^+e^-$  is excluded for  $\alpha_{\lambda\mu} - m_\lambda$  by  $g_\mu - 2$ .

The study of the  $\mu^+\mu^-$  mass spectrum in muon trident production,

$$\mu^\pm + N \rightarrow \mu^\pm + N' + \mu^+ + \mu^-, \quad (30a)$$

also provides a way to search for a muon-specific force. One would look for the process

$$\mu^\pm + N \rightarrow \mu^\pm + N' + \lambda, \quad \lambda \rightarrow \mu^+ + \mu^-, \quad (30b)$$

which would occur through a diagram similar to that in Fig. 12(b) with all  $e$ 's replaced by  $\mu$ 's. Sloan<sup>29</sup> has brought to our attention a study<sup>30</sup> of the  $\mu^+\mu^-$  mass spectrum from the reaction in Eq. (30a), the data having been obtained by the European Muon Collaboration.<sup>30</sup> There are no unexplained peaks in the  $\mu^+\mu^-$  mass spectrum. The upper limits which this null result imposes on  $\alpha_{\lambda\mu}$  have not been calculated.

We have already noted in Sec. V B 3 that we learn little new from  $e^+e^- \rightarrow \mu^+\mu^-$  compared to the joint limits from  $e^+e^- \rightarrow e^+e^-$  and  $g_\mu - 2$ . This assumes our model in which  $|\alpha_{\lambda e\mu}| = |\sqrt{\alpha_{\lambda e}\alpha_{\lambda\mu}}|$ . There may be more complex models which do not have this equivalence.

We are studying<sup>27</sup> data from PEP looking for the process

$$e^+ + e^- \rightarrow e^+ + e^- + \lambda, \quad \lambda \rightarrow \mu^+ + \mu^-. \quad (31)$$

This could take place through a Feynman diagram analogous to that in Fig. 12(a).

### 2. Possible future experiments

If the precision of the  $g_\mu - 2$  measurement is improved, then the unexplored region of  $\alpha_{\lambda\mu} - m_\lambda$  in Fig. 1(b) can be entered. The initial work leading to such an improvement has begun.<sup>31</sup>

Another way to extend the search for a  $\lambda$  which couples only to the  $\mu$  is to study the process in Eq. (30a) with increased statistics compared to Ref. 30. We have not

studied the sensitivity which could be achieved.

Other possible future experiments could explore the product  $\alpha_{\lambda e}\alpha_{\lambda\mu}$ . Extending the discussion in Sec. VI A 2, one could look for the process

$$e^- + p \rightarrow e^- + p + \lambda, \quad \lambda \rightarrow \mu^+ + \mu^-. \quad (32)$$

Or a deliberate energy scanning search could be made for a resonance in

$$e^+ + e^- \rightarrow \mu^+ + \mu^-. \quad (33)$$

From a broader viewpoint, there are still unresolved experimental questions concerning the production of muons when a high-energy  $e^-$  dissipates in a thick target. We refer to the work of Nelson and Kase<sup>32</sup> and of Nelson, Kase, and Svenson.<sup>33</sup> We do not know if the experimental results of these authors<sup>33</sup> have anything to do with the speculations in this paper. However a new high-energy study of

$$e^- + p \rightarrow \mu^+ + \mu^- + \dots$$

would help clarify those results

## C. $\tau$ specific forces

### 1. Remarks on limits and use of other data

The upper limit on  $\alpha_{\lambda e\tau}$  from  $e^+e^- \rightarrow \tau^+\tau^-$ , Fig. 11, gives an upper limit on the  $\alpha_{\lambda\tau}$  only if one assumes a relation between  $g_{\lambda e}$  and  $g_{\lambda\tau}$ . If the  $\lambda$  couples only to the  $\tau$ , there are two ways a  $\lambda$ - $\tau$  coupling could affect existing  $\tau$  data: (a) The  $\lambda$ - $\tau$  coupling would add to the  $\tau$ - $\gamma$ - $\tau$  vertex a correction term proportional to  $\alpha_{\lambda\tau}$ . The measurements of  $\sigma(e^+e^- \rightarrow \tau^+\tau^-)$  then limit the size of  $\alpha_{\lambda\tau}$ . (b) If  $m_\lambda < m_\tau$  there would be an effect on  $\tau$  decays proportional to  $\alpha_{\lambda\tau}$ . These two types of limits require some discussion of  $\tau$  physics and data and will be presented elsewhere.

### 2. Possible future experiments

We have no suggestions on how to better explore the limits on  $\alpha_{\lambda\tau}$  if the  $\lambda$  couples only to the  $\tau$ . Indeed little more can be done even if the  $\lambda$  also couples to the  $e$ . One cannot get much sensitivity from a search using

$$e^+ + e^- \rightarrow e^+ + e^- + \lambda, \quad \lambda \rightarrow \tau^+ + \tau^-; \quad (34)$$

there will not be a  $\tau^+\tau^-$  mass peak even if  $m_\lambda > 2m_\tau$ . The  $\tau$  remains a challenge to experimenters.

## ACKNOWLEDGMENTS

We appreciate discussions with E. M. Riordan and his very useful reading of our first draft. As always, Y. S. Tsai has been very helpful in providing theoretical insights and methods for calculation. We appreciate the discussions with, and support from, the members of the PEGASYS Collaboration. We appreciate discussions with W. R. Nelson on the production of muons by electron beams. We are grateful to T. Sloan for the information he provided on muon trident production. We thank H. A. Olsen for correcting an estimate in this paper. This work was supported by the Department of Energy, Contract No. DE-AC03-76SF00515.

- <sup>1</sup>H. -Y. Cheng, *Phys. Rev. D* **36**, 1649 (1987).
- <sup>2</sup>J. Reinhardt, A. Schäfer, B. Müller, and W. Greiner, *Phys. Rev. C* **33**, 194 (1986).
- <sup>3</sup>J. Steinberger, *Phys. Rev.* **76**, 1180 (1949).
- <sup>4</sup>V. W. Hughes, *Nucl. Phys. A* **463**, 3C (1987).
- <sup>5</sup>A. F. Rothenberg, Ph.D. thesis, Stanford University, Report No. SLAC-147, 1972. The experiment is briefly described in T. W. Donnelly *et al.*, *Phys. Rev. D* **18**, 1607 (1978).
- <sup>6</sup>J. D. Bjorken *et al.*, *Phys. Rev. D* **38**, 3375 (1988).
- <sup>7</sup>L. W. Mo (private communication).
- <sup>8</sup>Y. S. Tsai, *Phys. Rev. D* **34**, 1326 (1986).
- <sup>9</sup>W. R. Nelson, H. Hirayama, and D. W. O. Rogers, Report No. SLAC-PUB-4721, 1985 (unpublished).
- <sup>10</sup>The anomalous production of  $e^+e^-$  pairs by heavy ions is discussed in many papers in *Physics of Strong Fields*, edited by W. Greiner (Plenum, New York, 1980).
- <sup>11</sup>H. A. Olsen, *Phys. Rev. D* **36**, 959 (1987).
- <sup>12</sup>E. Holvik and H. A. Olsen, *Phys. Scr.* **38**, 324 (1988).
- <sup>13</sup>E. M. Riordan *et al.*, *Phys. Rev. Lett.* **59**, 755 (1987).
- <sup>14</sup>A. Konaka *et al.*, *Phys. Rev. Lett.* **57**, 659 (1980).
- <sup>15</sup>M. Davier *et al.*, *Phys. Lett. B* **180**, 295 (1986).
- <sup>16</sup>C. Brown *et al.*, *Phys. Rev. Lett.* **57**, 2101 (1986).
- <sup>17</sup>M. Davier, in *Proceedings of the XXIII International Conference on High Energy Physics*, Berkeley, California, 1986, edited by S. C. Loken (World Scientific, Singapore, 1987).
- <sup>18</sup>D. J. Bechis *et al.*, *Phys. Rev. Lett.* **42**, 1511 (1979).
- <sup>19</sup>M. Crisler *et al.*, Fermilab Proposal No. P774, 1986 (unpublished).
- <sup>20</sup>E. M. Riordan (private communication).
- <sup>21</sup>See, for example, S. L. Wu, *Phys. Rep.* **107**, 220 (1984).
- <sup>22</sup>M. Derrick *et al.*, *Phys. Rev. D* **34**, 3286 (1986).
- <sup>23</sup>M. Derrick *et al.*, *Phys. Rev. D* **31**, 2352 (1985).
- <sup>24</sup>K. K. Gan, Ph.D. thesis, Purdue University, 1985.
- <sup>25</sup>K. G. Hayes and M. L. Perl, *Phys. Rev. D* **38**, 3351 (1988).
- <sup>26</sup>A. Boyarski *et al.*, *Phys. Rev. Lett.* **34**, 762 (1975).
- <sup>27</sup>C. A. Hawkins and M. L. Perl (unpublished).
- <sup>28</sup>An  $e+p \rightarrow e+p+\lambda$  search is part of the PEGASYS proposal for studying general electroproduction of hadrons. The PEGASYS experiment would use the  $e^-$  beam in the PEP storage ring and a gas-jet target.
- <sup>29</sup>T. Sloan (private communication).
- <sup>30</sup>N. Dyce, Ph.D. thesis, University of Lancaster, 1988.
- <sup>31</sup>V. W. Hughes and G. T. Danby, in *Intersections between Particles and Nuclear Physics—1984*, proceedings of the Conference, Steamboat Springs, Colorado, edited by R. E. Mischke (AIP Conf. Proc. No. 123) (AIP, New York, 1984).
- <sup>32</sup>W. R. Nelson and K. R. Kase, *Nucl. Instrum. Methods* **120**, 401 (1974).
- <sup>33</sup>W. R. Nelson, K. R. Kase, and G. K. Svenson, *Nucl. Instrum. Methods* **120**, 413 (1974).